COBEM 2021 26th International Congress of Mechanical Engineering
November 22-26, 2021, Virtual Congress, Brazil

COB-2021-2329
BEAM CORRUGATED WITH MACRO FIBER COMPOSITE PATCHES FOR ACTIVE BAND GAP FORMATION

P. G. B. Oliveira
R. Nicoletti
C. Marqui Jr.
University of São Paulo, São Carlos School of Engineering, São Carlos-SP, 13566-590, Brazil
paulo.gustavo@usp.br, rnicolet@sc.usp.br, demarqui@sc.usp.br

Abstract. *Structures with geometric periodicity can present interesting dynamic properties like stop and pass frequency bands. This unusual dynamic behavior is also observed in corrugated beams due to their periodic geometry, with the advantage of having a constant cross-section area and material homogeneity (no need to change the mass or the material properties along the beam). Literature shows that, as we change the proportions of the bump (curved cell of the corrugated beam), the natural frequencies change and tend to open large band gaps in the frequency spectrum of the beam. The idea of the present work is to periodically attach macro fiber composite (MFC) actuators on the surface of a straight beam and control the corrugated geometry. Hence, it will be possible to actively create the band gaps in the structure by progressively changing its straight geometry to a corrugated one according to the input voltage level. In this work, we present the mathematical model of the beam and of the MFC patch, and we show numerically the effect of the patches on the frequency response functions of the beam: the beam starts presenting band gaps as we increase the action of the patches, by changing the geometry of the beam from a straight to a corrugated one.*

Keywords: *periodic structure, finite elements, mechanical vibration, natural frequency, metamaterial*

1. INTRODUCTION

Structures with some sort of periodicity can present interesting dynamic properties like stop and pass frequency bands (Wu and Song, 2018). One can take advantage of this phenomenon and design the structure to present a stop band (band gap) in a given frequency range, thus leading the structure to a low vibration response zone. That represents a passive way of controlling the structure vibration

Usually, the periodicity of the structure is achieved by imposing cross-section variations (Timorian *et al.*, 2019; Syed and Bishay, 2019) or material property variations (Syed and Bishay, 2019; Prasad and Sarkar, 2019). A variation of the stiffness can also impose periodicity on the structure, when the geometry or the material properties periodically vary along the structure (Pelat *et al.*, 2019; Alsaffar *et al.*, 2018). Another way of imposing the periodicity is by mounting resonators evenly distributed along the structure (Chouvion *et al.*, 2010; Xiao *et al.*, 2013; Hajhosseini and Ebrahimi, 2019). In this case, the resonators can be tailored to tune the band gap in specific frequency regions of the spectrum.

Recently, it has been observed that corrugated beams could also present band gaps in their frequency response if the curvature is repeated periodically (Nicoletti, 2020; Bachour and Nicoletti, 2021). Therefore, not only periodic variations of the cross-section, or periodic variations in the material properties, or the addition of periodically distributed resonators opens band gaps in the structure's response. By simply shaping the beam into a bumpy (corrugated) geometry (Fig. 1), one can also obtain attenuating effects (band gap formation), although due to a different mechanism. That represents a much simpler way of imposing periodicity in the structure to achieve desired dynamic effects.

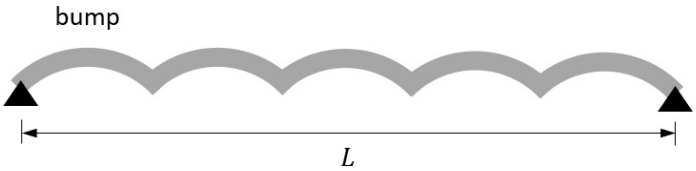

Figure 1. Periodically corrugated beam.

Considering this fact, there came the idea of imposing the corrugated geometry to the structure by active ways. In this sense, one could actively change the frequency response function of the structure, by imposing a corrugated geometry to

(a)  (b) 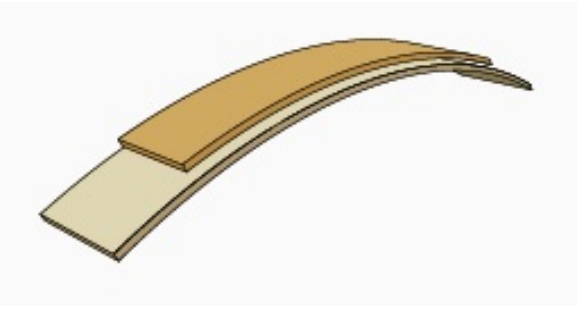

Figure 2. Macro Fiber Composite actuator produced by Smart Material Corp.: (a) actuator image, (b) bending actuation mode. (www.https://www.smart-material.com/MFC-product-mainV2.html)

the structure and, consequently, obtaining the band gaps in the response. A possible way of doing that is by mounting Macro Fiber Composite (MFC) actuators on the surface of the beam (Fig. 2).

In this work, we present the mathematical modeling of a beam mounted with MFC patches, aiming at actively changing its geometry from a straight to a corrugated one and obtaining a band gap region in the structure's response. The numerical results show that it is possible to achieve the desired corrugated geometry in the beam, and consequently the band gaps, by turning on the actuators mounted on the structure. However, the structure must present low bending stiffness, like those of thin metallic sheets.

2. MATHEMATICAL MODELING

2.1 Corrugated Beam

The beam is modeled with Finite Elements. Each element has two nodes and each node has three degrees of freedom: axial displacement (u), transverse displacement (v), and angular displacement ($\theta = dv/du$). These degrees of freedom are related to the local coordinate system of the element (u, v), as shown in Fig. 3. Therefore, to obtain the governing equations of the whole beam in the global coordinate system (X, Y), one needs to perform a coordinate transformation.

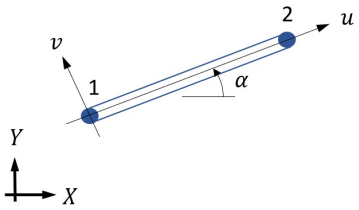

Figure 3. Global and local coordinates of the finite element used to model the corrugated beam.

The inertia ($\mathbf{M}_e$) and the stiffness ($\mathbf{K}_e$) matrices of this finite element, based on the Euler-Bernoulli theory, are provided by Thomson and Dahleh (1998) and presented in the Appendix. The authors also provide the transformation matrix $\mathbf{T}(\alpha)$ necessary for obtaining the global matrices of the model. By performing the coordinate transformation:

$$\mathbf{M}_e^G = \mathbf{T}^T(\alpha)\,\mathbf{M}_e\mathbf{T}(\alpha) \tag{1}$$

$$\mathbf{K}_e^G = \mathbf{T}^T(\alpha)\,\mathbf{K}_e\mathbf{T}(\alpha) \tag{2}$$

one obtains the inertia and stiffness matrices of the element in global coordinates. By modeling the whole beam as a series of connected finite elements, and compiling all the element global matrices, one derives the global equations of motion of the beam modeled by these finite elements:

$$\mathbf{M}\ddot{\mathbf{q}} + \mathbf{K}\mathbf{q} = \mathbf{f} \tag{3}$$

where $\mathbf{M}$ and $\mathbf{K}$ are the global inertia and stiffness matrices of the model, $\mathbf{q}$ is the vector of degrees of freedom in global coordinates, and $\mathbf{f}$ is the vector of external forces.

The frequency response function of the beam is obtained by calculating the receptance matrix of the system. For that, we assume a harmonic response $\mathbf{q} = \mathbf{Q}\,e^{i\omega t}$ due to a harmonic excitation $\mathbf{f} = \mathbf{F}\,e^{i\omega t}$. Hence, the receptance matrix $\mathbf{H}(\omega)$ is given by:

$$\mathbf{H}(\omega) = \left(-\omega^2\mathbf{M} + \mathbf{K}\right)^{-1} \tag{4}$$

The element $H_{i,j}(\omega)$ of the receptance matrix will give the frequency response function of the system at the i-th degree of freedom due to an excitation at the j-th degree of freedom of the system.

2.2 Macro Fiber Composite Actuator

The MFC actuator is composed of thin PZT (lead zirconate titanate) fibers of rectangular cross section, separated by epoxy layers (Fig. 4a). Electrodes transversely mounted to the PZT fibers impose the electric field necessary to activate the PZT fibers, which expand or contract depending on the polarization of the electrodes. The properties of the MFC are usually provided for a single cell of the system, called Representative Volume Element (RVE) – Fig. 4b. The RVE commprises the volume of a PZT fiber between two electrodes.

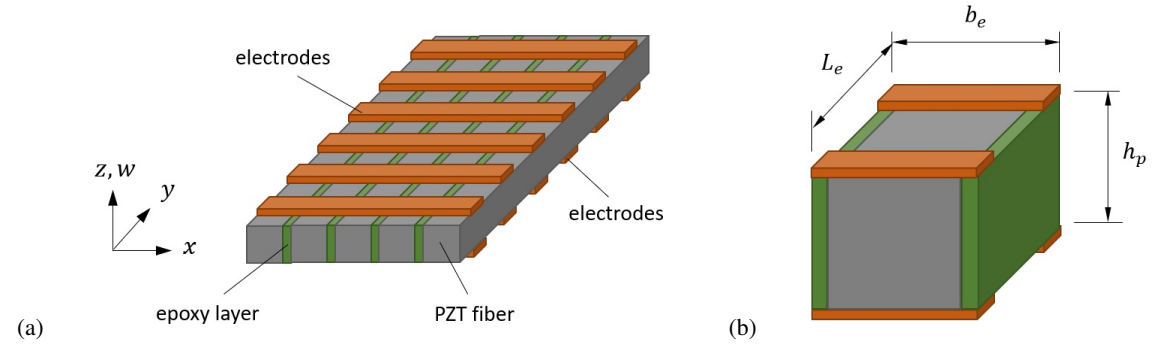

Figure 4. Macro Fiber Composite (MFC): (a) internal structure with PZT fibers and electrodes, (b) the Representative Volume Element (RVE).

We can model the MFC actuator as an Euler-Bernoulli beam (Shahab and Erturk, 2017), whose equation of motion is given by:

$$\rho_m A_m \frac{\partial^2 w}{\partial t^2} - \frac{\partial^2 M}{\partial x^2} = 0 \tag{5}$$

where ρ_m is the MFC density, A_m is the MFC cross-section area, $w(x,t)$ is the transverse displacement, and M is the internal bending moment, given by:

$$M = \int_A T_3 z \, dA = \sum_{i=1}^{N_L} \sum_{j=1}^{N_W} b_e \int_{-hp/2}^{hp/2} T_3 z \, dz \tag{6}$$

where N_L is the number of RVEs in the longitudinal direction of the MFC, N_W is the number of PZT fibers in the width direction of the MFC, b_e is the width of the RVE, h_p is the PZT thickness, and T_3 is the mechanical stress.

The linear constitutive equations of the RVE with 33-mode coupling is given by Erturk and Inman (2011):

$$T_3 = c_{33}^E S_3 - e_{33} E_3 \tag{7}$$

where c_{33}^E is the equivalent elastic modulus at a constant electric field, S_3 is the strain, e_{33} is the effective piezoelectric stress constant, and E_3 is the electric field.

The strain in the MFC is given by:

$$S_3 = -z \frac{\partial^2 w}{\partial x^2} \tag{8}$$

whereas the electric field in the RVE is:

$$E_3 = \frac{v(t)}{L_e} \tag{9}$$

where $v(t)$ is the electric voltage applied to the electrodes, and L_e is the distance between two electrode fingers.

Hence, by inserting Eqs.(7), (8), and (9) into Eq.(6), solving the integral, and inserting it into Eq.(5), one derives the electromechanically coupled equation of the MFC, as follows:

$$\rho_m A_m \frac{\partial^2 w}{\partial t^2} + c_{33}^E I_m \frac{\partial^4 w}{\partial x^4} = \vartheta v(t) \left[\frac{d\delta(x)}{dx} - \frac{\delta(x-L)}{dx} \right] \tag{10}$$

where I_m is the cross-section area moment of inertia of the MFC, $\delta(.)$ is the Dirac delta, L is the total length of the MFC, and ϑ is the electromechanical coupling, given by:

$$\vartheta = N_W \, d_{33} \, c_{33}^E \frac{A_e}{L_e} \tag{11}$$

where one assumed that $e_{33} = d_{33} \, c_{33}^E$ (Erturk and Inman, 2011; Shahab and Erturk, 2017), d_{33} is the piezoelectric charge constant, and A_e is the cross-section area of the PZT fiber ($A_e = b_e \, h_p$).

2.3 Model Coupling

By looking at the equation of motion of the MFC (Eq.(10)), we see that the left-hand side represents the equation of an Euler-Bernoulli beam. The loading applied to this beam is in the right-hand side of the equation, represented by the forces caused by the piezoelectric effect, applied at the extremities of the beam. Hence, considering that the MFC is represented by the model of an Euler-Bernoulli beam, we can also use the Finite Element Method described in section 2.1 to model the MFC. In this case, one must consider that the MFC is mounted over the base structure, as shown in Fig. 5. The inertia and rigidity of the MFC (left-hand side of Eq.(10)) will be considered in the model by adding the finite element matrices of inertia and stiffness of the MFC to the base structure model (Eq.(3)). The forces caused by the piezoelectric effect (right-hand side of Eq.(10)) will be transferred to the nodes of the base structure model (nodes that coincide with the extremity nodes of the MFC model), taking into account the distance between the center lines of the base structure and the MFC.

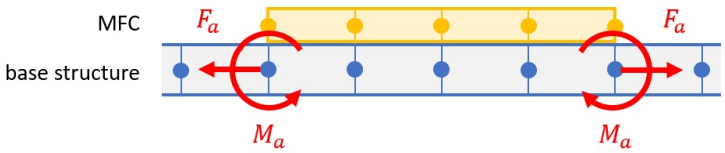

Figure 5. Representation of the finite element modeling of the base structure with the MFC.

Hence, the axial force exerted by the MFC on the base structure is given by:

$$F_a = \vartheta \, v(t) \tag{12}$$

whereas the bending moment applied by the MFC to the base structure is given by:

$$M_a = N_L \, \vartheta \, v(t) \, h_a \tag{13}$$

where $h_a = (h_s + h_m)/2$, h_s is the base structure thickness, and h_m is the MFC thickness.

It is important to highlight that, in this approach, we are neglecting the shift of the neutral line in the finite elements of the MFC. However, considering that both the MFC and the base structure have thicknesses of tenths of millimeters, such assumption will not significantly affect the results.

3. NUMERICAL RESULTS

In this work, we will adopt the MFC model 8528 of the Smart Material Co. The dimensions of this MFC is shown in Fig. 6 and its parameters are listed in Table 1. The MFCs are periodically mounted on the top surface of an aluminum beam. In the present study, we adopted 6 MFCs as shown in Fig. 7, and the beam is fully constrained at its extremities (fully constrained boundary conditions). The properties of the beam are listed in Table 2.

According to the mathematical model presented in section 2.3, the MFCs will add inertia and stiffness to the beam at their respective locations along the beam. That is usually overlooked in more massive and rigid structures. However, as it will be later shown in this section, we need slender structures to achieve the desired results of shaping the beam in a corrugated way by using the MFCs. Therefore, in the present case, the amount of inertia and stiffness added by the MFCs to the structure is important.

By looking at Fig. 7, we have 6 active elements (MFCs) adding mass and inertia to the structure in a periodic way. This alone can induce band gaps in the structure without applying any electric voltage to the MFCs. To check this effect, we varied the thickness of the base structure (aluminum beam) and calculated the resultant natural frequencies of the system, without applying any voltage to the MFCs. The results are presented in Fig. 8, where the dots are the natural frequencies ω_n of the system normalized by the fundamental frequency ω_0. The colors in Fig. 8 refer to the frequency response function (FRF) of the beam, where the excitation was applied at the first unconstrained node of the model and the response was calculated at the last unconstrained node of the model.

Table 1. Parameters of the MFC model 8528 (Shahab and Erturk, 2017).

parameter	*value*	*unit*
number of RVEs in the longitudinal (N_L)	185	—
number of PZT fibers in the width (N_W)	72	—
width of PZT fiber (b_e)	0.356	mm
height of PZT fiber (h_p)	0.180	mm
distance between two electrodes (L_e)	0.407	mm
equivalent elastic modulus (c_{33}^E)	43.78	GPa
piezoelectric charge constant (d_{33})	437	pm/V
width of MFC (active area)	28	mm
length of MFC (L)	85	mm
thickness of MFC (h_m)	0.300	mm
density of MFC (ρ_m)	7,500	kg.m^{-3}

Table 2. Parameters of the beam.

parameter	*value*	*unit*
beam width	30	mm
beam length	1020	mm
beam thickness	0.5 / 1.0	mm
Young modulus	69	GPa
material density (ρ)	2,700	kg.m^{-3}

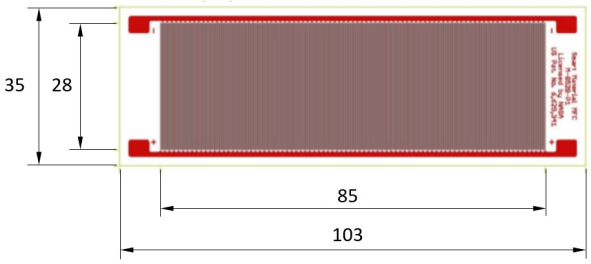

Figure 6. Dimensions of the MFC model 8528 in millimiters. (https://www.smart-material.com/MFC-product-P1V2.html)

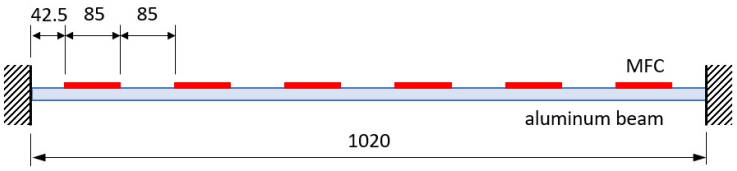

Figure 7. Aluminum beam with 6 MFCs periodically mounted on the top surface (in mm).

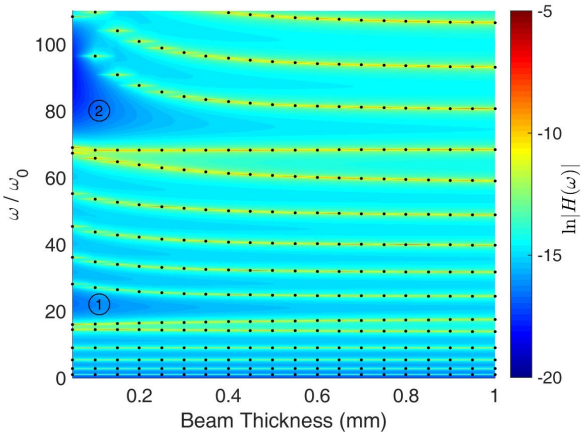

Figure 8. Natural frequencies (dots) and the amplitude of the FRF (colors) of the beam with 6 MFC actuators as a function of the thickness of the beam (null voltage applied to the MFCs).

As we can see in Fig. 8, the structure starts to present band gaps (regions ① and ②) when the beam has thicknesses below 0.4 mm. Hence, to check the effectiveness of the proposed method (i.e. create band gaps by turning on the MFCs), we must adopt beams that do not already present band gaps, e.g. with thicknesses above 0.4 mm.

Figure 9a presents the natural frequencies and the FRF of the beam with 0.5 mm thickness. In this case, we varied the

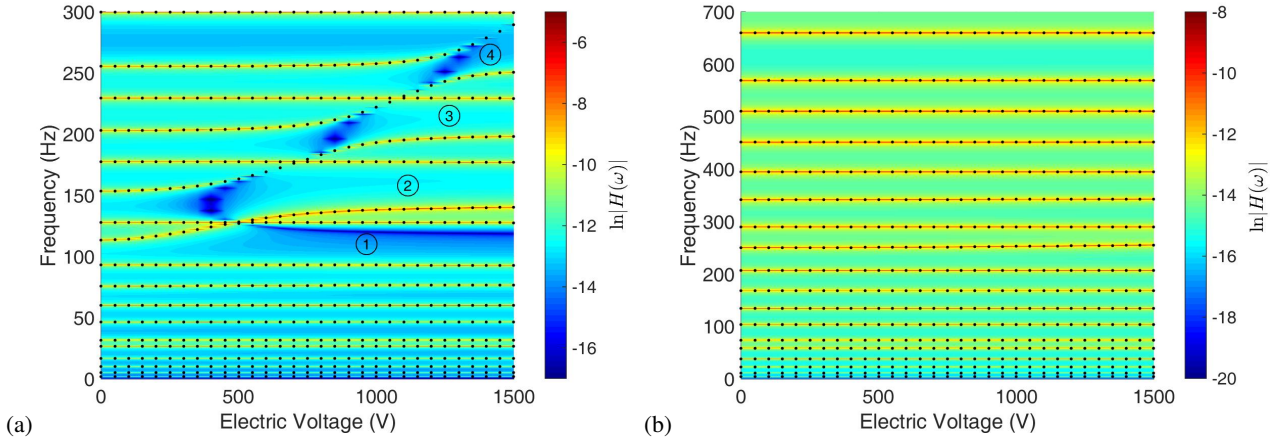

Figure 9. Natural frequencies (dots) and the amplitude of the FRF (colors) of the beam with 6 MFC actuators as a function of the electric voltage applied to the MFCs: (a) beam with 0.5 mm thickness, (b) beam with 1 mm thickness.

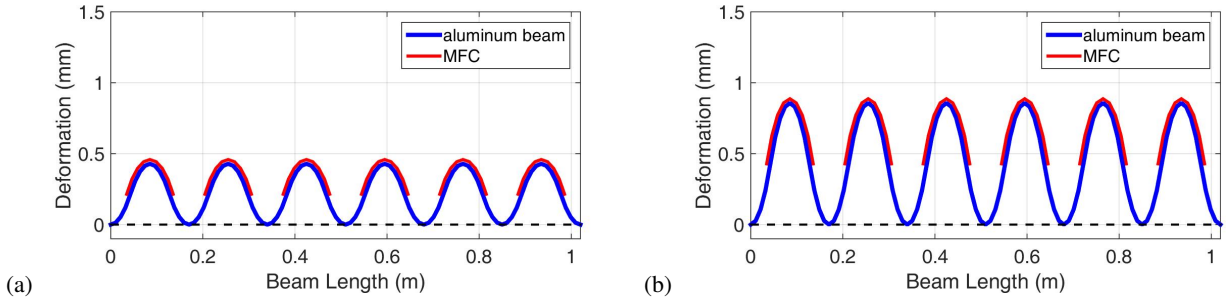

Figure 10. Deformation of the beam when the MFCs are turned on: (a) 750 V, (b) 1,500 V.

electric voltage applied to the MFCs from 0 to 1,500 V (equal voltage applied to all MFCs). As we can see, as the voltage increases, the MFCs increase their force and gradually deform the beam in a corrugated way (Fig. 10). As a consequence, some natural frequencies start to shift towards higher frequency ranges, thus leaving modal gaps in the spectrum (regions ① , ②, ③ and ④in Fig. 9a). This is an expected effect, as previously reported in literature (Bachour and Nicoletti, 2021), where the number of bumps in the structure define the natural frequencies that shift. The natural frequencies of the corrugated beam with curved bumps shift as the cut-off frequency associated to the longitudinal waves increases and crosses the odd natural frequencies (Nicoletti, 2020).

Hence, it is possible to create band gaps in the frequency spectrum of the beam by using MFCs by deforming it in a corrugated way. However, the force of the MFC is not high and that represents an important limitation in terms of practical applications. For example, if we increase the thickness of the beam to 1.0 mm, the deformation of the beam caused by the MFCs is not big enough to result in a shifting of the natural frequencies of the system (Fig. 9b). As a consequence, no band gaps form in the spectrum of the structure, and the MFCs are ineffective. In this case, the base structure is too stiff to be sufficiently deformed by the MFCs to present the frequency shifting effect of a corrugated beam.

4. CONCLUSION

In this work, we presented the mathematical modeling of a beam with Macro Fiber Composite (MFC) actuators mounted on it. In the numerical simulations, we analyzed the effects of the MFCs on the natural frequencies of the system. The main conclusions are:

- it is possible to create band gaps in the frequency spectrum of beams by using MFCs and deforming it in a corrugated way;
- the effectiveness of the system depends on the stiffness of the base structure. The present design solution is more suitable for slender structures;
- if the structure is too slender (low stiffness), the sole presence of the MFCs lead the system to present band gaps.

The numerical results presented in this work shall be confirmed by experimental data as a natural next step of the research.

5. ACKNOWLEDGEMENTS

This project was supported by the Brazilian research foundations FAPESP (Fundação de Amparo à Pesquisa do Estado de São Paulo), under grant no. 2018/15894-0 (ENVIBRO Project), and CNPq (Conselho Nacional de Desenvolvimento Científico e Tecnológico), under grants no. 301118/2018-3, 433456/2018-3, and 308690/2019-2.

6. APPENDIX

The finite element matrices of the Euler-Bernoulli beam with three degrees of freedom per node are (Thomson and Dahleh, 1998):

$$\mathbf{M}_e = \frac{\rho\, l_e}{420}\begin{bmatrix} 140 & 0 & 0 & 70 & 0 & 0 \\ & 156 & 22\,l_e & 0 & 54 & -13\,l_e \\ & & 4\,l_e^2 & 0 & 13\,l_e & -3\,l_e^2 \\ & & & 140 & 0 & 0 \\ & \text{sym.} & & & 156 & -22\,l_e \\ & & & & & 4\,l_e^2 \end{bmatrix} \tag{14}$$

where ρ is the material density, and l_e is the length of the element.

$$\mathbf{K}_e = \frac{E\,I}{l_e^3}\begin{bmatrix} R & 0 & 0 & -R & 0 & 0 \\ & 12 & 6\,l_e & 0 & -12 & 6\,l_e \\ & & 4\,l_e^2 & 0 & -6\,l_e & 2\,l_e^2 \\ & & & R & 0 & 0 \\ & \text{sym.} & & & 12 & -6\,l_e \\ & & & & & 4\,l_e^2 \end{bmatrix} \tag{15}$$

where E is the material's Young modulus, I is the cross-section moment of inertia, A is the cross-section area, and $R = A\,l_e^2/I$.

The matrix of transformation of coordinates, necessary to transfer the element local coordinates to the global system of coordinates, is:

$$\mathbf{T}(\alpha) = \begin{bmatrix} \cos\alpha & \sin\alpha & 0 & & & \\ -\sin\alpha & \cos\alpha & 0 & & \text{zeros} & \\ 0 & 0 & 1 & & & \\ & & & \cos\alpha & \sin\alpha & 0 \\ & \text{zeros} & & -\sin\alpha & \cos\alpha & 0 \\ & & & 0 & 0 & 1 \end{bmatrix} \tag{16}$$

where α is the angle of the element in relation to the global coordinates.

7. REFERENCES

Alsaffar, Y., Sassi, S. and Baz, A., 2018. "Band gap characteristics of periodic gyroscopic systems". *Journal of Sound and Vibration*, Vol. 435, pp. 301–322. doi:10.1016/j.jsv.2018.07.015.

Bachour, R.S. and Nicoletti, R., 2021. "Natural frequencies and band gaps of periodically corrugated beams". *Journal of Vibration and Acoustics*, Vol. 143, p. 044502. doi:10.1115/1.4048889.

Chouvion, B., Fox, C.H.J., McWilliam, S. and Popov, A.A., 2010. "In-plane free vibration analysis of combined ring-beam structural systems by wave propagation". *Journal of Sound and Vibration*, Vol. 329, pp. 5087–5104. doi: 10.1016/j.jsv.2010.05.023.

Erturk, A. and Inman, D.J., 2011. *Piezoelectric energy harvesting*. John Wiley and Sons, Chichester.

Hajhosseini, M. and Ebrahimi, S., 2019. "Analysis of vibration band gaps in an euler–bernoulli beam with periodic arrays of meander-shaped beams". *Journal of Vibration and Control*, Vol. 25, No. 1, pp. 41–51. doi: 10.1177/1077546318768995.

Nicoletti, R., 2020. "On the natural frequencies of simply supported beams curved in mode shapes". *Journal of Sound and Vibration*, Vol. 485, p. 115597. doi:10.1016/j.jsv.2020.115597.

Pelat, A., Gallot, T. and Gautier, F., 2019. "On the control of the first bragg band gap in periodic continuously corrugated beam for flexural vibration". *Journal of Sound and Vibration*, Vol. 446, pp. 249–262. doi:10.1016/j.jsv.2019.01.029.

Prasad, R. and Sarkar, A., 2019. "Broadband vibration isolation for rods and beams using periodic structure theory". *Journal of Applied Mechanics*, Vol. 86, p. 021004. doi:10.1115/1.4042011.

Shahab, S. and Erturk, A., 2017. "Coupling of experimentally validated electroelastic dynamics and mixing rules formulation for macro-fiber composite piezoelectric structures". *Journal of Intelligent Material Systems and Structures*, Vol. 28, No. 12, pp. 1575–1588. doi:10.1177/1045389X16672732.

Syed, M. and Bishay, P.L., 2019. "Analysis and design of periodic beams for vibration attenuation". *Journal of Vibration and Control*, Vol. 25, No. 1.

Thomson, W.T. and Dahleh, M.D., 1998. *Theory of vibration with applications*. Prentice Hall, Upper Saddle River, 5th edition.

Timorian, S., Petrone, G., Rosa, S., Franco, F., Ouisse, M. and Bouhaddi, M., 2019. "Spectral analysis and structural response of periodic and quasi-periodic beams". *Journal of Mechanical Engineering Science*, Vol. 233, No. 23–24, pp. 7498–7512. doi:10.1177/0954406219888948.

Wu, L.J. and Song, H.W., 2018. "Band gap analysis of periodic structures based on cell experimental frequency response functions (frfs)". *Acta Mechanica Sinica*, Vol. 35, No. 1, pp. 156–153. doi:10.1007/s10409-018-0781-0.

Xiao, Y., Wen, J., Wang, G. and Wen, X., 2013. "Theoretical and experimental study of locally resonant and bragg band gaps in flexural beams carrying periodic arrays of beam-like resonators". *Journal of Vibration and Acoustics*, Vol. 135, p. 041006. doi:10.1115/1.4024214.

8. RESPONSIBILITY NOTICE

The authors are solely responsible for the printed material included in this paper.